Lecture 12 : Clusters of galaxies

All sky surveys in the later half of 20th century changed the earlier view that clusters of galaxies are rare and that only a small fraction of galaxies are grouped together into structures. A handful of clusters like Virgo and Coma were of course studied in detail. A pioneering study by Abell (1958, ApJS, 3, 211) found 2712 rich clusters on the Palomer survey plates, a sample that is still used (together with the 1989 supplement, there are now 4073 rich clusters). Abell's criterion for a cluster was to have at least 50 members in the magnitude range (m_3, m_3+2) (with the magnitude m_3 of the 3rd brightest galaxy) within the Abell radius, $R_A + 1.7/(1+z) \sim 3h_{50}^{-1}$ Mpc. He classified the clusters according to the number of cluster members (N) and their density. A richness class 0 ($30 < N < 49$), class 1 ($50 < N < 79$) and so on to class 5 ($N \geq 300$) were thus defined.

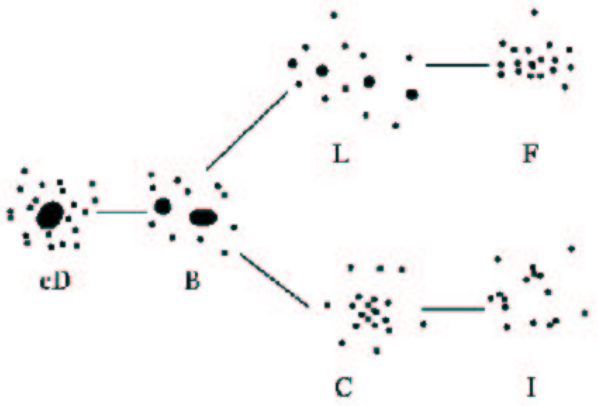

Figure 1: Rood-Sastry classification scheme.

There is another scheme of classification that is in vogue, called the Rood-Sastry system (1971), which can be described briefly as follows: **cD**–the cluster is dominated by a central cD galaxy (e.g., A2199); **B**–the cluster is dominated by a pair of luminous galaxies (e.g., Coma); **L**–the luminous galaxies are in a linear array (e.g., Perseus); **C**–the cluster has a single core (e.g, Corona Borealis, A2065); **F**–has a flattened distribution (e.g., Hercules); **I**–the distribution is irregular (e.g., A400). Usually one depicts these classes in a tuning-fork pattern.

Figure 2: There are two central cDs in Coma cluster, at a distance of ~ 100 Mpc. There is a sub-cluster in the SW region which is perhaps in the process of merging with Coma.

1 Dynamics and mass

The standard method of estimating the masses of clusters, which are self-gravitating systems, is using the virial theorem. To recapitulate, if one assumes equal masses of bodies, then differentiating $I = \frac{1}{2} m \Sigma R_i^2$ twice with respect to time one gets, $\ddot{I} = m\Sigma_i \ddot{\mathbf{R}}_i \cdot \mathbf{R}_i + m\Sigma_i \dot{\mathbf{R}}_i^2$. The second term is the twice the kinetic energy T, and the first term is the potential energy $m\Sigma_i \ddot{\mathbf{R}}_i \cdot \mathbf{R}_i = -Gm^2 \Sigma_i \Sigma_{i \neq j} \frac{(\mathbf{R}_i - \mathbf{R}_j)\cdot \mathbf{R}_i}{R_{ij}^3} = -Gm^2 \Sigma_i \Sigma_{j<i} \frac{1}{R_{ij}} = W$, where $R_{ij} = |\mathbf{R}_i - \mathbf{R}_j|$. Taking a time average, denoted by $\langle \rangle_t$, for a system in steady state ($\langle \ddot{I} \rangle_t = 0$), one has, $-Gm^2 \Sigma_{i<j} \langle 1/R_{ij} \rangle_t + m\Sigma_i \langle V_i^2 \rangle_t = 0$. Taking an average over all possible orientation, denoted by $\langle \rangle_\Omega$, one has $\langle V_i^2 \rangle_\Omega = 3 \langle V_{zi}^2 \rangle_\Omega$, and $\langle R_{ij}^{-1} \rangle_\Omega = 2/\pi \langle R_{\perp,ij}^{-1} \rangle_\Omega$. Therefore, in the case of equal masses, for N cluster members, one has

$$M = \frac{3\pi N}{2G} \frac{\Sigma_i \langle V_{zi}^2 \rangle_{t,\Omega}}{\Sigma_{i<j} \langle 1/R_{\perp,ij} \rangle_{t,\Omega}} \,. \tag{1}$$

The typical masses are found to be 10^{15} solar masses for rich clusters. It is found that the total mass estimated by virial theorem is in excess of what is expected from their optical luminosity. It is found that M/L is typically $(100 - 500)\frac{M_\odot}{L_\odot}$. Historically, this was the first indication of the presence of dark matter.

The velocity dispersion $\sigma = (\Sigma V_i^2)^{1/2}$ is of order of 1000 km/s for rich clusters. The sizes involved are a few Mpc, so the crossing time is of order $10^9 (R/Mpc)(\sigma/1000 km/s)$ yr.

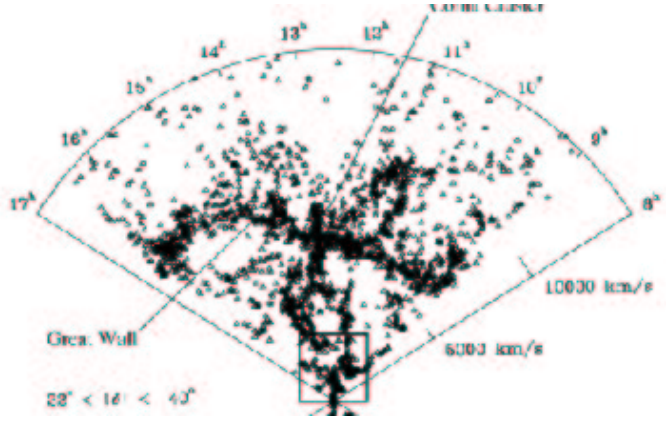

Figure 3: The redshift-position diagram showing the position of Coma cluster (da Costa, Geller and Huchra.

It is reasonable to assume that on this large scale, different components of mass have not separated during the collapse, and therefore clusters of galaxies are representative samples of the universe. When we compare later the baryonic and dark matter content of the universe, we will argue that this should be close to the universal value.

Also clusters are a part of the hierarchy of structures in the universe, with a typical overdensity of $\Delta\rho/\bar{\rho} \sim 10^3$. The richest clusters are usually found at the intersections of sheets and filamets of the large scale structures of the universe. For example, Coma is situated at an intersection in the Great Wall (see the CfA galaxy survey).

2 Member galaxies

2.1 Morphology-Density relation

It was as early as in 1926 that Shapely noticed the different galaxy content of Virgo and Coma cluster, Coma being dominated by spheroidal galaxies. Tombaugh noticed ten year later that cluster ellipticals are more centrally concentrated than cluster spirals. Dressler finally showed in a classic paper in 1980 (ApJ, 236, 351) that (1) regular as well as irregular clusters display the same morphology-density relation and that (2) the local density determines the morphology mix at a given radius of a cluster. He showed that the fractional variation of ellipticals with the

projected density has a negative slope, unlike those of spirals and SOs.

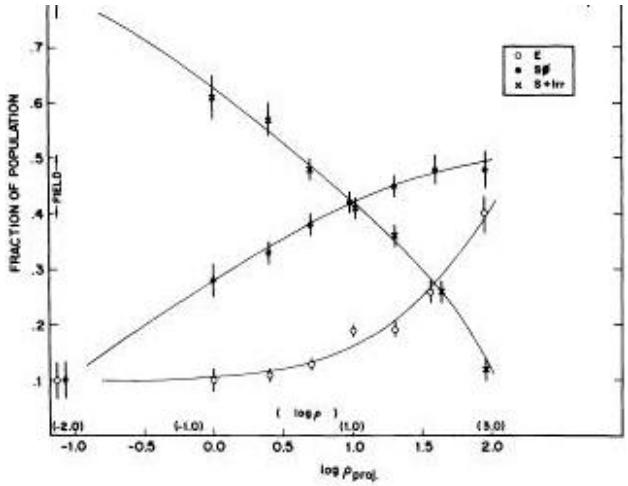

Figure 4: The fraction of E, SO, and S+I galaxies as a function of the log of the projected density (in galaxies per cubic Mega parsecs) is shown, as in Dressler's 1980 paper.

We have of course seen this in the difference of Luminosity functions of galaxies in field and clusters. Essentially the spiral/elliptical ratio is lower in clusters than in the field. It is still unclear whether or not this relation is due to something that happened during the formation or evolution of galaxies. It is possible that spirals may be stripped of gas to make SOs (from ram pressure stripping; see below). Simulations by Moore et al (1996) have shown that spirals going through 'galaxy harrassment' can resemble SOs, and spiral mergers may also create SOs and Es.

3 Intracluster gas

A significant amount of matter in cluster resides in diffuse gaseous form. It was discovered in 1970s with the Uhuru satellite that there are many clusters that radiated in X-ray with $L_x \sim 10^{43}$–10^{45} erg/s. The spectra is well fitted by thermal bremsstrahlung of a hot gas with $T \sim 10^7$–10^8 K. For cosmic abundance one has for bremsstrahlung (for a 7 keV gas, say),

$$L_X \sim 2.4 \times 10^{-27} \mathrm{erg/s} \int n_e^2 dV \tag{2}$$

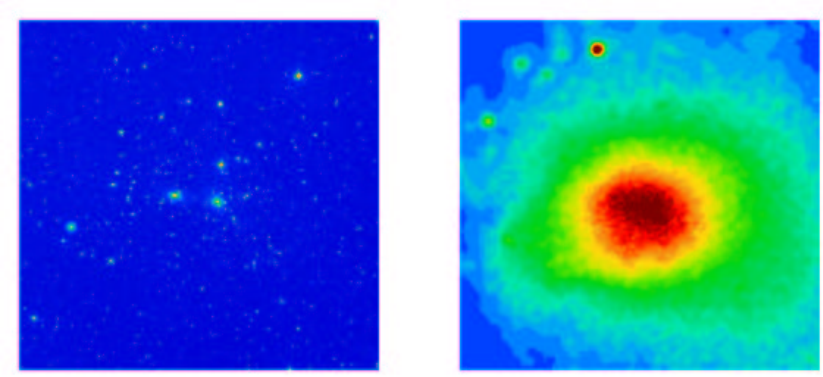

Figure 5: Coma in optical and Xray.

The temperature is close to that expected from galaxy velocity dispersion, $kT \sim m_p\sigma^2$ which means that the origin of the thermal energy of the gas is tied up with the background gravitational potential of the cluster, as is the velocity dispersion of galaxies. In other words, $(3/2)kT \sim m_p\phi$.

One can easily determine the temperature of the gas from the shape of the spectrum. The observed intensity then (assuming a physical lengthscale) then gives the particle density. The typical density in rich clusters is $\sim 10^{-3}$ cm^{-3}. This also indicates a total gas mass. It turns out that the total gas mass is comparable to that of member galaxies in poor clusters, but it is several times that of galaxy masses for rich clusters. Typically one has $M_{gas} \sim 5M_{gals}$.

Homework on ram pressure stripping : see Shu

There are some emission lines in addition to the continuum and one can infer the presence of highly ionized heavy elements like iron. The transitions take place in the inner shells (e.g., n=1,2 (K,L)). The temperatures derived from degree of ionization is consistent with that derived from continuum shape : suggests that gas is collisionally ionized. The typical abundance is of order $1/3$ solar, and it is hardly dependent on the total cluster mass. For very poor groups, there is still some uncertainty in the measurement of the metallicity. This indicates that ram pressure is not important for the enrichment of ICM, otherwise there would be a dependence on cluster temperature (Renzini 1997).

There is a small metallicity gradient, with metallicity decreasing outwards, as was found from high resolution spectroscopy with ASCA.

The origin of this metallicity is still uncertain, although the general idea is that galactic winds from member galaxies has enriched it. There is a good corre-

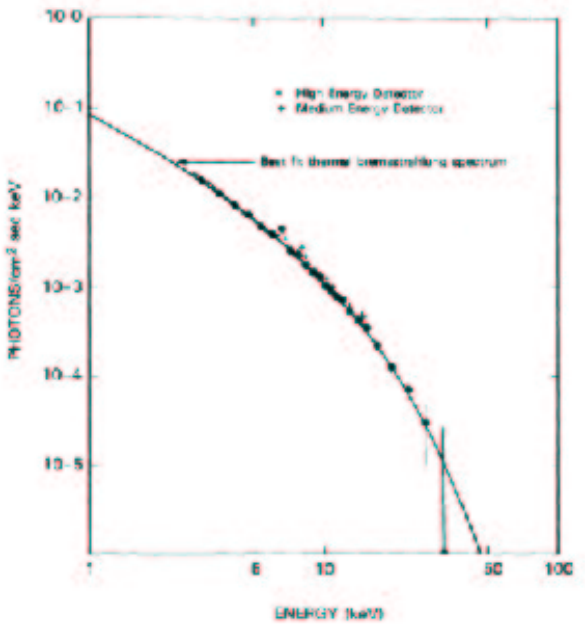

Figure 6: X-ray spectrum of Coma cluster shows that

lation between the mass in metals with the luminosity (or equivalently, mass) of spheroids (E and SOs), suggesting that the source of galactic winds are the ellipticals in clusters. The overall relative abundance is that of SN II type, with the ratio between Si and Fe being on the higher side.

An interesting correlation between Si/Fe ratio and the cluster temperature (Fukazawa et al 1998, PASJ, 50, 187) show that cooler clusters have ratios characteristic of SN Ia (Si/Fe being low), whereas hot clusters have ratios close to SN II (high Si/Fe). SN I's take a while to dominate the supernova rate in a galaxy, depending on the evolution of binary stars, whereas in the beginning core collapse supernovae, SN II's, dominate. This indicates that massive cluster have retained most of the ejects from from the initial burst of SN II, while most of the metals in poor clusters come from recent SN Ia.

It is found that the mass in metals in the ICM is comparable to that in galaxies ($M_Z(ICM) \sim M_Z(gals)$). It perhaps means that galaxies have lost a significant fraction, of order 50%, of their initial gas content in winds. If we now recall that the gas mass is 3-5 times that mass in galaxies, it is reasonable to say that a large part of the ICM gas is primordial and has not come from galaxies.

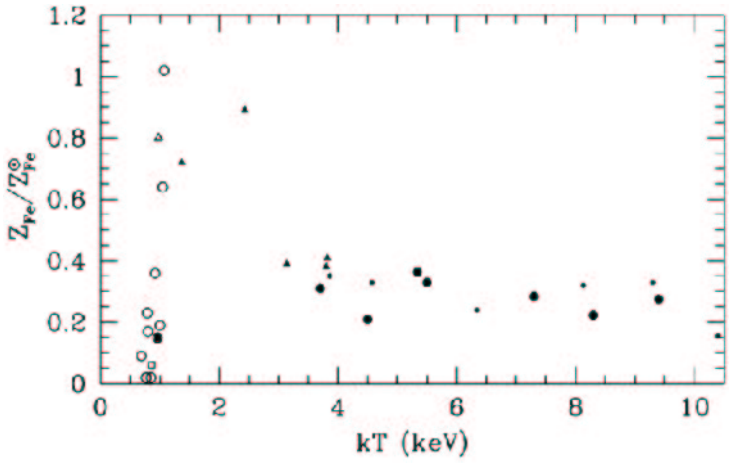

Figure 7: ICM metallicity (with iron as tracer) vs cluster temperature.

3.1 Cooling flows

The rather high density in the central region of ICM implies that the gas there cools very fast. In fact, about 2/3 of all rich clusters have densities such that $t_{cool} \propto nkT/n^2T^{1/2} \leq 10^{10}$ yr within 100 kpc. In the absence of any balancing heating sources, the gas is expected move inward because of outer pressure, and steepen the density profile. The expected rise in luminosity, and the fall in temperature, is seen in many clusters. The temperature does not however fall below 1-2 keV. One needs a heating source in the centre to model this properly, and AGN sources have been invoked.

3.2 Entropy

Although the temperature of the gas is understood from gravitational potential that the gas finds itself in, it is not easy to explain the gas density that clusters have. There is evidence that gas distribution in poor clusters is shallower than in rich clusters. One uses the concept of 'entropy' in describing this. Defining entropy as $T/n_e^{2/3}$, it appears that the entropy, at a fixed scaled radius, say 10% of the total radius of the cluster, is *larger* for poor cluster than what is expected if the gas density is simply proportional to the dark matter density. This has been interpreted as being a sign of non-gravitational energy input in the ICM, especially of poor clusters.

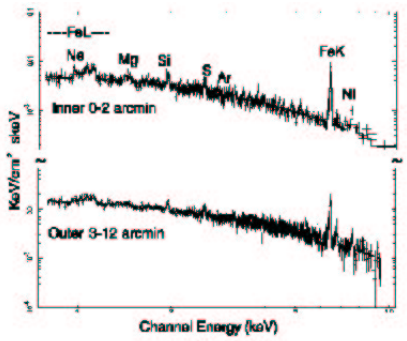

Figure 8: A spectra of the inner and outer regions of Abell 496 (Dupke and White 2000, ApJ,537,123)

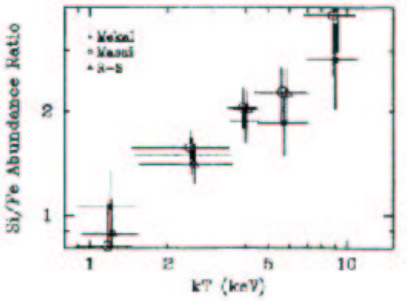

Figure 9: Correlation between Si/Fe ratio with Cluster temperature.

4 Mass estimates

One can estimate the total mass of cluster by using the X-ray observations of the hot gas and assuming it to be in hydrostatic equilibrium with the background potential (assuming it to be of trace quantity, not contributing to the potential). Using ideal gas relation of $p = nkT$, one can write the hydrostatic equilibrium condition as,

$$\frac{GM_{tot}(<r)}{r} = -\frac{kT}{\mu m_p}\left(\frac{d\ln\rho_g}{d\ln r} + \frac{d\ln T}{d\ln r}\right). \tag{3}$$

Assuming spherical symmetry one can use the observed distribution of $\rho_g(r)$ and $T(r)$ to obtain the total mass profile.

One can also use gravitational lensing obseravtions to determine the total mass. The matter in cluster acts as a lens for the distant bakcground galaxies. One can in principle invert the observed distortions of background galaxies to ob-

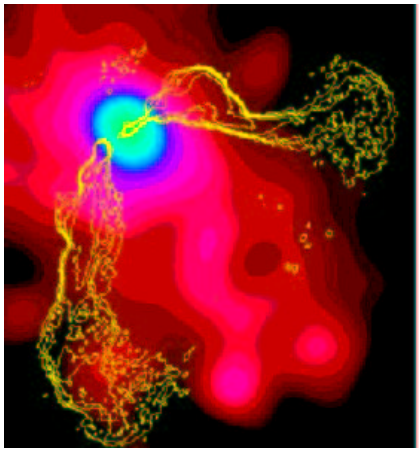

Figure 10: The interaction between radio galaxies and the ICM gas is an interesting topic of research. This 'tailed' radio galaxy is associated with the central galaxy of Abell 2634. The X-ray image is superposed on radio contours (Owen and Eilek).

tain the mass profile, given high resolution images that are now easily available (after HST). It is interesting that both estimates of mass profile agree to a large extent.

5 Sunyaev-Zel'dovich effect

The hot ICM gas also shows up as holes in the microwave sky, since it inverse-Compton scatters the microwave background radiation photons. This interaction (originally predicted by Sunyaev and Zel'dovich in 1969) scatters the Rayleigh-Jeans photons into the Wien's side of the spectrum, thereby decreasing the intensity in the RJ part of the spectrum. The extent of the interaction is expressed by the Compton 'y' parameter defined as,

$$y = \frac{k_B T_e}{m_e c^2} n_e \sigma_T L, \tag{4}$$

, where T_e is the temperature of the electrons, n_e is their number density and L is the size of the gaseous system. It can be shown that in the R-J part the fractional decrement of the microwave flux, $dI/I \sim 2y \sim 10^{-5}$, for $n \sim 10^{-3}$ cm^{-3} and $T \sim 5 \times 10^7$ K, and $L \sim 200$ kpc. The interesting aspect of SZ effect is that the

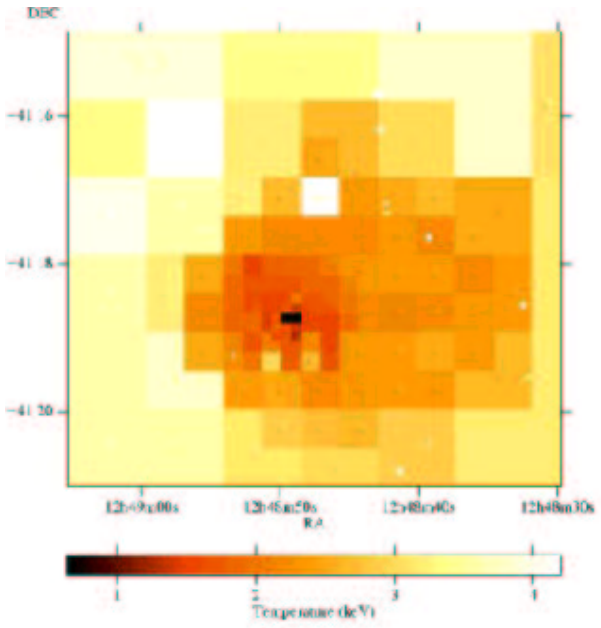

Figure 11: The temperature map of Centaurus cluster (Abell 3526; Sanders and Fabian 2001), showing cooler gas at the central region.

decrement is independent of the distance and therefore can be used to discover and study gas in high redshift clusters.

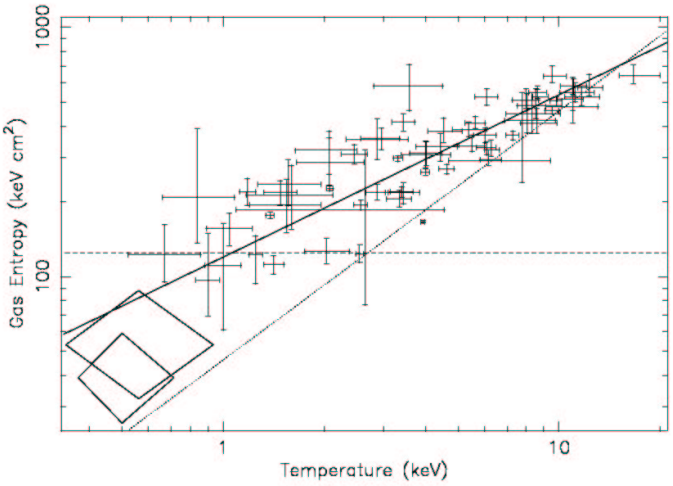

Figure 12: Entropy at $0.1R_{200}$ of clusters compared to the self-similar expectations (Ponman et al 2003).

Figure 13: HST image of Abell 2218 showing the distortions of the background galaxies.

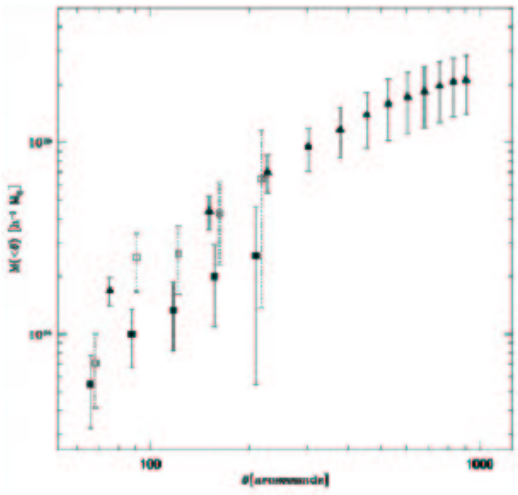

Figure 14: The radial mass profile of Abell 2163 determined from X-ray (triangles) and lensing analysis (open squares). (Squires et al 1997, ApJ, 482, 648)

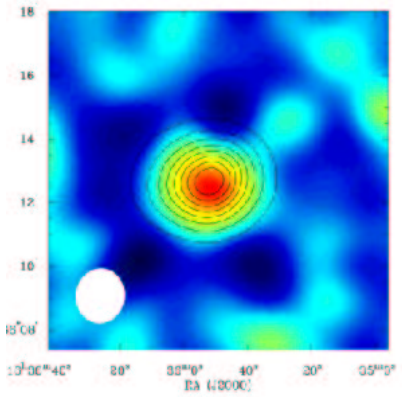

Figure 15: SZ effect (in colour) at 28.5 GHz against the cluster Abell 2218. The ROSAT X-ray image is shown with contours (Carlstrom et al).